The University of South Bohemia in České Budějovice

Faculty of Science

Subcellular localization analysis of proteins non univocally located to the mitochondria of *Trypanosoma brucei*

Bachelor thesis

Stina Eßmann

Advisor: Ignacio Durante, Ph.D

Co-Advisor: Mgr. Vendula Rašková

České Budějovice 2021

Eßmann S., 2021: Subcellular localization analysis of proteins non univocally located to the mitochondria of *Trypanosoma brucei*. Bc. Thesis, in English, -49 p., Faculty of Science, University of South Bohemia, České Budějovice, Czech Republic.

Annotation

In this thesis *in situ* tagging by parasite transfection, followed by Western Blot and immunofluorescence microscopy was performed for the analysis of the endogenous localization of prioritized *Trypanosoma brucei* proteins. The prioritized non univocally located proteins had TrypTag.org annotations that corresponded or were compatible with tripartite attachment complex (TAC). For the determination of essentiality, RNAi constructs were generated by Gibson assembly molecular cloning.

Declaration

I declare that I am the author of this qualification thesis and that in writing it I have used the sources and literature displayed in the list of used sources only.

Place, date: České Budějovice, 18.08.2021
Student's signature:

Contents

Abbreviations

APRT	Adenine phosphoribosyl transferase
BSFs	Bloodstream forms/trypomastigotes
CT	C-terminally
CYT	cytoplasm
DAPI	4′,6-diaminido-2-phenylindol
DNA	deoxyribonucleic acid
dNTPs	deoxynucleotides triphosphate
E. coli	*Escherichia coli*
gDNA	genomic DNA
GI	Gene Identifier
HAT	Human African Trypanosomiasis
HSP70	Heat Shock Protein 70
IFA	Immunofluorescence assay
kDNA	kinetoplast DNA
min	minutes
MIT	mitochondria
mNG	mNeonGreen
NT	N-tagged
PBS	Phosphate buffered saline
PBS-T	Phosphate buffered saline + Polysorbate 20 (0,05% V/V)
PCFs	Procyclic forms
PCR	Polymerase Chain Reaction
PVDF	Polyvinylidene fluoride
RNAi	ribonucleic acid interference
RT	room temperature
SDS	Sodium Dodecyl Sulphate
SDS-PAGE	Sodium Dodecyl Sulphate-Polyacrylamide Gel Electrophoresis
T. brucei	*Trypanosoma brucei*

TAC	Tripartite attachment complex
vPBS	Vorheis’ modified PBS
WCL	Whole cell lysate
x	times

Acknowledgment

I want to express my enormous gratitude towards Professor Sterba and Professor Grubhoffer for supporting me in any concern throughout this project, listening to my problems, and helping to solve them.

I am furthermore incredibly grateful to Mgr. Vendula Rašková who guided me throughout the whole project and supported me in performing the experiments.

Moreover, I am very thankful for the support and love obtained by my family. Without them, this thesis would not have been possible.

1 Introduction

1.1 *Trypanosoma brucei's* medical relevance and its cell cycle

Trypanosoma brucei (*T. brucei*) is a flagellated protozoan and causative agent of Human African Trypanosomiasis (HAT) and *nagana* in cattle. *T. brucei* belongs to the class of Kinetoplastea, which is comprising several other parasites causative of human and zoonotic diseases of superlative sanitary relevance. Further examples of Trypanosomes would include *Trypanosoma cruzi* causing the American Trypanosomiasis or Leishmaniases caused by distinct *Leishmania* spp (Barrett et al., 2003).

The subspecies of *T. brucei* causing HAT are *T. brucei gambiense* and *T. brucei rhodesiense*, while *T. brucei brucei* affects wild and domestic animals. Other species, non-pathogenic to humans, are *T. congolense*, and the causative agents of durine and surra diseases in camels and horses, *T. brucei evansi* and *T .brucei equiperdum*, respectively (Brun et al., 2010).

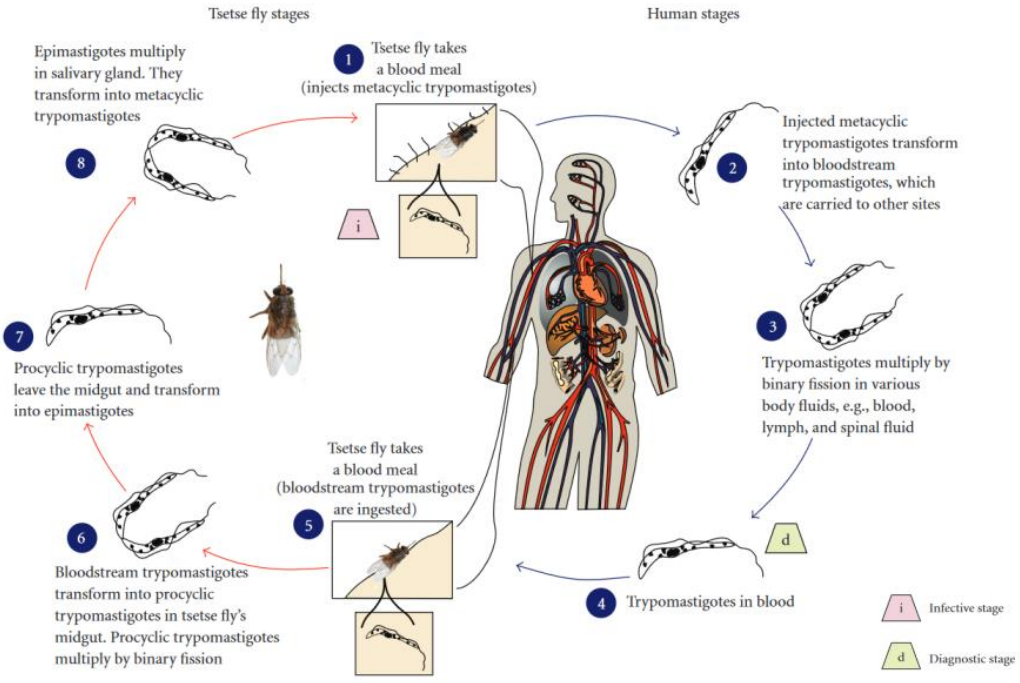

Figure 1. Life cycle of African Trypanosomes. By taking a blood meal tsetse fly inoculates metacyclic trypomastigotes into the human body where the parasites further evolve to bloodstream forms (stages1,2,3,4). This bloodstream forms are then ingested again by the tsetse fly (stage 5) where they convert to procyclic cells within the midgut of the fly (stage 6) followed by evolving into epimastigotes on their way to the fly's salivary gland (stage 7). Within the salivary gland they replicate by binary fission and convert to metacyclic trypomastigotes again (Baral, 2010).

T. brucei exhibits a very complex life cycle in which it copes with the diverse and rapidly changing environmental conditions when alternating between the insect (tsetse fly) and the mammalian host (human) (see Figure 1). *T. brucei's* life cycle starts within the fly's organism, in which its bloodstream trypomastigotes (BSFs) convert into procyclic trypomastigotes (PCFs), followed by their reproduction by binary fission. Afterward, these PCFs access the fly's midgut and alter into epimastigotes, followed by their further outstretch to the fly's salivary glands, where they differentiate into metacyclic trypomastigotes infective to the mammal host. (Brun et al., 2010). These metacyclic trypomastigotes colonizing the tsetse fly or invertebrate host are transferred to the mammal host during a blood meal. Within the human bloodstream, these metacyclic trypomastigotes further transform into BSFs and reach out to other body parts like adipose tissue, where they replicate by binary fission. BSFs are then re-transferred to the invertebrate host during the next blood meal, where the life cycle begins again.

1.2 Cellular specializations and complexity

As well as other trypanosomatids, *T. brucei* is a highly complex cell bearing specialized cell organelles that allows the cell to cope with environmental conditions and developmental transitions during the life cycle of *T. brucei*.

An example of this, is *T. brucei's* exclusive peroxisome-related glycosome devoted to glycolysis (Parsons, 2004). Throughout the different developmental stages of the protist's life cycle, glycosomes adjust their enzymatic composition in response to their exposed environmental conditions. Thus, the enzymatic composition within this organelle is highly dynamic. In particular 90% of glycosomal enzymes in BSFs are committed to glycolysis, while PCFs can switch between glycolysis, amino-acid catabolism, and the tricarboxylic acid cycle as a source of energy transference molecule Adenosine triphosphate production. Therefore, only around 50% of glycosomal enzymes in PCFs are eventually involved in glycolysis (Bauer & Morris, 2017).

Furthermore, to be mentioned, and highly relevant for this thesis, is the large single mitochondrion present within *T. brucei* cells, which is composed out of ca. 1008 proteins identified under a variable degree of confidence (Panigrahi et al., 2009). It is like the glycosome, a highly dynamic organelle, also suffers extensive remodeling during *T. brucei's* life cycle. It is exhibiting relatively abundant and diminished *cristae* in PCFs and BSFs, respectively, partly reflecting the transitions regarding energetic metabolism: from oxidative phosphorylation in PCFs to substrate-level phosphorylation in BSFs (Bílý et al., 2021).

Another characteristic mitochondrial feature of *T. brucei* and in general of all kinetoplastids is the possession of kinetoplast, composed of catenated maxi- and minicircles of mitochondrial or kinetoplast deoxyribonucleic acid (kDNA) connected into a large network (Ogbadoyi et al., 2003). During genome segregation, the kDNA is connected to basal bodies by the Tripartite Attachment Complex (TAC), named according to its dispersal across the cell (see Figure 2). This special TAC complex is ensuring the correct genome distribution of the beforehand replicated kDNA into the corresponding daughter cells within a dividing cell (Baudouin et al., 2020).

The maintenance of the kDNA during replication, as well as the correct segregation of the genetic material during cell division, is crucial for proper cell division and survival in *T. brucei* (Hoffmann et al., 2018).
Up to now, only a few proteins in *T. brucei* (e.g., p166, p197, TAC40, and TAC102) are assumed to display a TAC like subcellular distribution together with a monoclonal antibody (Mab22) localized within the exclusion zone filaments of TAC that constitutes as a marker for the cytoplasmic region of the complex (Schneider & Ochsenreiter, 2018). Further components of the TAC would include the differentiated mitochondrial membranes and the unilateral filaments.

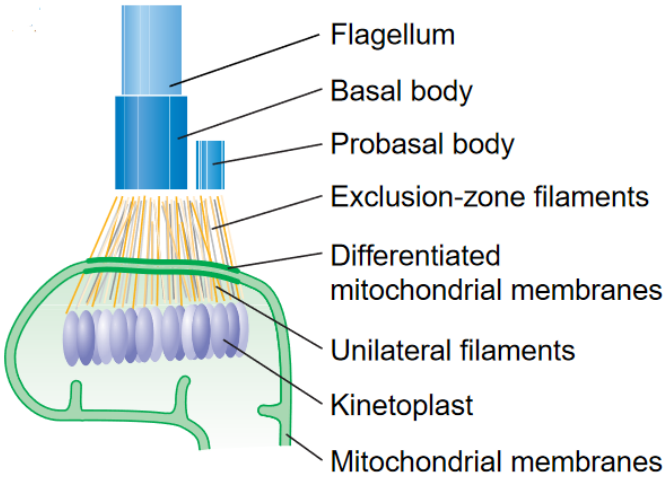

Figure 2: TAC structure and its components. The basal and probasal bodies are indicated in blue, Unilateral filaments/Exclusion-zone filaments are shown in yellow/grey, Kinetoplast DNA is shown in purple and mitochondrial membranes are indicated in green (Liu et al., 2005).

Other components of the TAC are:

The protein p166, which is assumed to be localized within the area between the mitochondrial inner membrane and the kDNA. p166 is exhibiting an N-terminal mitochondrial targeting sequence together with a potential transmembrane domain, not being necessary for its localization but may be influencing or affecting the protein's function (Hoffmann et al., 2018; Zhao et al., 2008).

TAC102, which is the kDNA's most proximal component is lacking an N-terminal mitochondrial targeting sequence, and C-terminal targeting signals are required for TAC sorting between the kDNA and the basal body of the flagellum (Trikin et al., 2016).

TAC40 is a beta-barrel protein within the porin family. Its function is exclusively restricted to mitochondrial genome segregation, and the protein is being localized within the outer mitochondrial membrane (Hoffmann et al., 2018; Schnarwiler et al., 2014).

p197 is assumed to be a TAC element within *T. brucei* when being present in its PCFs. Till now, it is still unclear if p166 and p197 are as well crucial in *T. Brucei* BSFs and if their properties are strictly limited to mitochondrial-genome segregation. p197 is assumed to be localized in between the exclusion zone filaments of the complex (Hoffmann et al., 2018).

The monoclonal antibody Mab22 was determined to be localized in the exclusion zone filaments as well as in the mature and probasal body (Hoffmann et al., 2018; Bonhivers et al., 2008). It is directed against a yet still unknown protein (Schneider & Ochsenreiter, 2018).

Depletion of these TAC components was associated with defects in the growth of procyclic as well as in bloodstream forms and/or kDNA segregation during cell division (Schneider & Ochsenreiter, 2018). So far, TAC restricted proteins have only been linked to mitochondrial genome segregation and were not compromising any other supplementary functions.
Furthermore, TAC complex itself is assumed to be congregated in a hierarchical manner beginning at the base of the flagellum and then directed towards the mitochondrial genome, whereby its assembly is not regulated by the kDNA itself. The complex seems to be composed out of multiple nonoverlapping subcomplexes and is assumed to compromise an overall molecular weight of around 2.8 MDa. The TAC itself plays an important role in the correct mitochondrial organelle positioning but is not required for the mitochondrial organelle biogenesis and segregation (Hoffmann et al., 2018).

1.3 Genome annotation

Due to the medical and economic relevance of *T. brucei*, the genome of the protist, as well as related trypanosomatid genomes, have been extensively sequenced (Baudouin et al., 2020). These sequenced genomes are now available in the genome database TriTrypDB, accessible for further characterization, especially for investigating the obtained proteomic data in the post-genomic era (Aslett et al., 2009). For this purpose, the TrypTag.org project was created, which is a project aiming to determine the subcellular localization of every beforehand sequenced protein within Trypanosomes utilizing N- and/or C-terminal endogenous tagging followed by microscopic investigation and publishing the results online.
By taking advantage of the localization data available on TrypTag.org, identification of several candidates for a more detailed investigation that were determined to be mitochondrial and putatively related to TAC was performed. Intending to identify yet novel TAC proteins, we performed an in-silico based prioritization of proteins with dual, non-univocal localization as determined by TrypTag.org and assessed their localization through Immunofluorescence assay (IFA) and Western Blot analysis of subcellular fractionations. Further, the essentiality was assessed by using ribonucleic acid interference (RNAi).

1.4 Prioritization and preliminary analysis

Prioritization of the selected proteins was carried out by our supervisor based on a bibliographic assessment of the previous characterization. Therefore, the available localization data on TrypTag.org was checked for proteins, which got tagged C-terminally as well as N-terminally with mNeonGreen throughout the project and showed a dual subcellular localization (To investigate the processes in TAC during genome segregation proteins compromising a dual localization with a possible TAC like distribution were prioritized). Furthermore, the available micrographs (Figure 3) on the TrypTag.org database of these same proteins exhibiting a dual localization were inspected to evaluate the possible TAC-like distribution signals. Moreover, their assumed assigned functions and/or domains due to sequence similarity to other proteins were evaluated.

As a result, the following candidates were chosen for a more detailed investigation (Table 1):

GI[a]	Description[b]	Prosite[c]	Superfamily[d]	NT[e]	CT[f]
Tb927.2.5020	acyl-CoA oxidase, putative	N/A	Acyl-CoA dehydrogenase C-terminal domain-like;Acyl-CoA dehydrogenase NM domain-like	CYT	TAC
Tb927.6.1570	2-hydroxy-3-oxopropionate reductase, putative	N/A	6-phosphogluconate dehydrogenase C-terminal domain-like;NAD(P)-binding Rossmann-fold domains	CYT	TAC
Tb927.8.1440	maoC-like dehydratase, putative	N/A	Thioesterase/thiol ester dehydrase-isomerase	CYT	TAC, CYT
Tb927.8.6970	3-methylcrotonyl-CoA carboxylase alpha subunit, putative	Biotinyl/lipoyl domain profile;ATP-grasp fold profile;Biotin carboxylation domain profile	Single hybrid motif;Rudiment single hybrid motif;PreATP-grasp domain;Glutathione synthetase ATP-binding domain-like	CYT	TAC

Table 1: The GIs (Gene Identifiers) of the final candidates proposed for characterization is shown. [a] : Gene identifier, [b] : names of proteins as annotated in TriTrypDB, [c] : domains annotated in Prosite, [d] : Superfamily annotation, [e] : N-terminal Neon Green tagging and obtained localization results of the proteins, [f] : C-terminal mNG tagging (TrypTag.org) and obtained localization results. Abbreviations: CYT; cytoplasm, MIT; mitochondrion, K; kinetoplast, TAC; tripartite attachment complex, N.D.; not

For all selected proteins, a “TAC-like” associated distribution of the fluorescent signal in all C-terminally (CT) tagged candidates and a cytoplasmic expression of NT-mNG fused constructs was found, suggesting that NT tagging may abolish some NT translocation signals to the TAC. Many other hypothetical proteins not included here displayed the same pattern of behaviour bearing putative N-terminal signal peptides or targeting sequences possibly for translocation into the TAC. CT tagged mNG products were also found to display dual localization, associated

in some cases with mitochondrial (MIT) and cytoplasmic (CYT) compartments in addition to TAC-related localization.

All selected proteins bear either Prosite or Superfamily homology inferred putative domains, which can, in turn, be linked to important biological processes. Thus, the distinct NT/CT localization was prompting to validate whether the selected candidates were indeed TAC related.

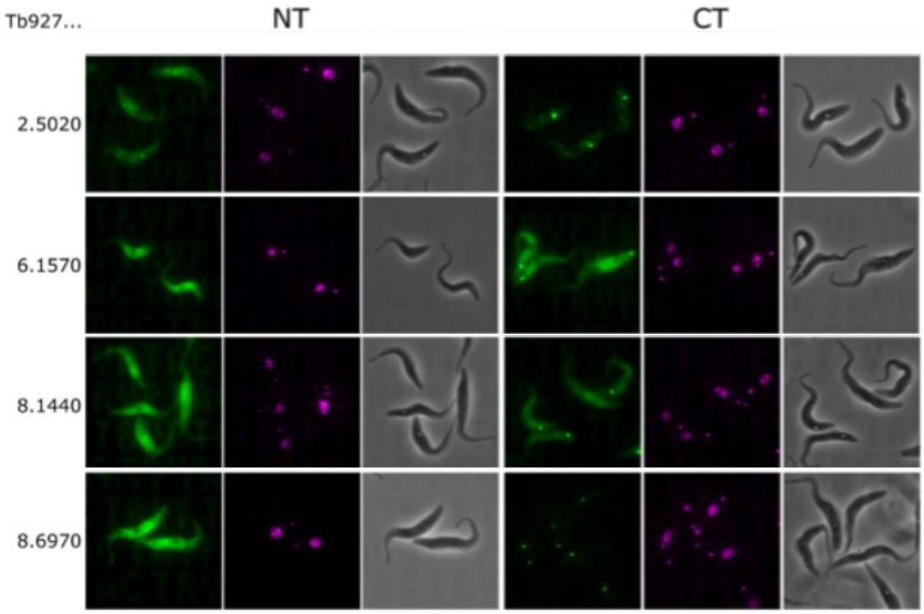

Figure 3: TrypTag.org micrographs corresponding to the prioritized candidates indicated by GI. Purple signal displaying nucleic stained genetic material by Hoechst, green signal displaying tagged proteins by mNG, grey pictures displaying the phase contrast of the cells. All selected proteins exhibited cytoplasmic staining when N-terminally tagged (NT) and TAC-like localization when C-terminally tagged.

Throughout further investigations, the aim was to prevent interference with NT translocation signals, and therefore endogenous tagging was only performed in a C-tagged manner. In contrast to the TrypTag.org procedure, where the bulky mNG is used for tagging, a smaller V5 tag was preferred. During IFA, 4’,6-diamidine-20-phenylindole dihydrochloride (DAPI) was used instead of Hoechst (another stain used to stain genetic material within the nucleus of a cell).

2 Aim of the work

The aim of the project was to determine the subcellular localization of the prioritized *T. brucei* genes Tb927.2.5020 (acyl-CoA oxidase), Tb927.6.1570 (2-hydroxy-3-oxopropionate reductase), Tb927.8.1440 (maoC-like dehydratase), and Tb927.8.6970 (3-methylcrotonyl-CoA carboxylase alpha subunit) by in situ-tagging with CT V5-tagged versions of the proteins using a pPOT based strategy. Over these obtained cell lines fine localization assessment by IFA and further Western Blot analysis over CYT/MIT subcellular fractionations were performed. Additionally, constructs for monitoring the effects of the ablation/knock down of the expression of the candidates' products by RNAi were generated and the growth phenotype of Tb927.8.1440 was evaluated.

3 Materials and Methods

3.1 Polymerase Chain Reaction

The Polymerase Chain reaction (PCR) is a biological method to amplify specific DNA regions by performing distinct temperature-dependent reactions.
During a classic PCR, the fragment to be amplified, known as template DNA, is mixed with several components like deoxynucleoside triphosphates (dNTPs), heat-stable DNA-polymerases (usually from *Thermus aquaticus* bacterium), and a mixture of primers. This primer mixture is compromising forward primers complementary to the starting sequence of the template DNA. In contrast, the reverse primers complement the end of the sequence to be amplified (Sambrook et al., 1989).

A PCR reaction, and thus the amplification of the target DNA, is usually performed based on five distinct steps. Initialized is the reaction by heat activating the DNA polymerase (hot-start PCR) if required. Afterward, the denaturation step follows. Next, the double-stranded DNA fragments are separated into single strands by breaking the hydrogen bonds due to roughly heating the mixture for a few seconds. Primers are then allowed to anneal to these single-stranded DNA fragments under the appropriate annealing temperature. Upon successful primer annealing, strand elongation is initialized under the operating temperature of the used polymerase. Finally, the overall PCR reaction is terminated by a final elongation, ensuring that all amplified DNA fragments are fully extended.

Throughout this project, PCR reactions were performed to amplify the inserts for cloning of RNAi constructs, create the stuffers to generate long hairpin in Gibson assembly, and amplify the pTrypSon backbones with opposing primers.

3.2 In-situ tagging and cloning of RNAi constructs

3.2.1 Preparation of RNAi plasmids

To design tetracycline-inducible RNAi cell lines, PCR reactions of the gene regions of interest over genomic DNA (gDNA) were performed (for PCR conditions see appendix) based on the following reaction mix:

Component	amount
Q5 hotstart	25 µL
Water	23 µL
Corresponding forward primer	1 µL
Corresponding reverse primer	1 µL
gDNA	1 µL

Obtained PCR products were evaluated by agarose gel electrophoresis and were further purified using the Nucleospin Gel and PCR clean-up kit (Macherey-Nagel, Germany). Purified products were then mixed with the stuffer, the plasmid backbone, Milli-Q water, and the Gibson assembly master mix for further Gibson assembly reaction (for exact compositions, see appendix).

Therefore, the Gibson assembly reaction mixes were incubated at 50°C for 1h to generate long hairpin RNAi constructs. Gibson assembly products were further processed by transforming them into *E. coli* (*Escherichia coli)* XL-1 blue bacteria. To verify the correct assembly of the RNAi constructs by Gibson assembly colony PCR was performed.

Therefore, obtained colonies from the transformation procedure were transferred to a fresh ampicillin petri dish and were resuspended in 8 ul of sterile Milli-Q water, followed by cell lysis (Table 2).

Table 2: Cell lysis program used before colony PCR:

96°C	5’
50°C	1’30’’
96°C	1’30’’
45°C	1’
96°C	1’
40°C	1’
4°C	2’

Lysed colonies (8 µL) afterward were mixed with BioPPPMMix (10 µL) supplemented with 1 µL of forwarding specific primer and 1 µL genomic RNAi reverse primer (see appendix). Reaction mixtures were then inserted into the thermal cycler and were exposed to colony PCR conditions (Table 3).

Table 3: PCR conditions for colony PCR:

94°C	2’	
94°C	20’’	15x
65°C (-1°C per cycle)	30’’	
72°C	1’15’’	
94°C	20’’	20x
50°C	30’’	
72°C	1’15’’	
72°C	7’	
12°C	12’	

Afterward, products were checked by agarose gel electrophoresis to ensure their correct size, followed by cultivation in LB media supplemented with ampicillin. Purification of the plasmids with correct inoculated inserts was performed by using the NucleoSpin Miniprep (General). Plasmid linearization was obtained due to the application of the NotI-HF restriction enzyme. The obtained DNA constructs were validated by sequencing prior to transfection into PCF *T. brucei* cells to obtain stable RNAi cell lines.

3.3 Preparation of V5 tagged cell lines

To C-terminally tag the selected proteins *in situ*, forward and reverse primers with a total length of approximately 100 nucleotides were designed. Forward primers thereby were created to contain at least 80 nucleotides in 5' to 3' direction out of the open reading frame before the stop codon of the target gene. This sequence is then followed by the first approximately 20 nucleotides out of the plasmid backbone preceding the tag sequence. The reverse primer was designed for compromising the reverse complement of the first 80-100 nucleotides of the 3' untranslated region of the target gene in 5' to 3' direction, accompanied by approximately 20 nucleotides of the plasmid backbone immediately downstream of the antibiotic resistance gene (Dean et al., 2015; Oberholzer et al., 2005).

The primers were then further processed in PCR together with a pPOTv5 vector (a modified vector in which YFP present in the original (parental) pPOTv4 vector was replaced by a 3xV5 epitope, allowing for C-Terminal V5 tagging (Figure 5)) serving as templates to produce the long primer amplicon, compromising the tag as well as the selective marker. Afterward, the obtained PCR results were analysed by agarose gel electrophoresis (for reaction Mix and PCR conditions, see appendix).

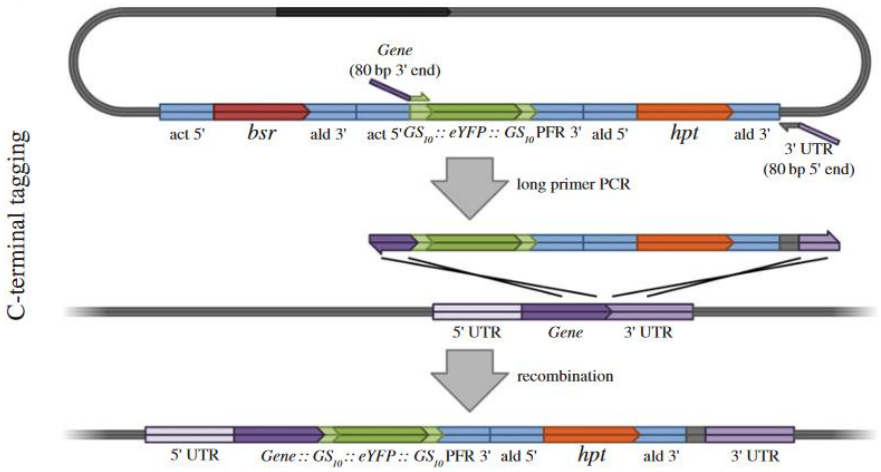

Figure 4: C-terminal long primer PCR tagging and deletion mutagenesis using pPOTv4 (Dean et al., 2015)

Confirmed products were further transfected into procyclic *T. brucei* SMOX cell lines and recombined in a way that the tag was combined to the target gene (performed by supervisor). Recombinant cell lines were selected by using the appropriate drug (performed by supervisor).

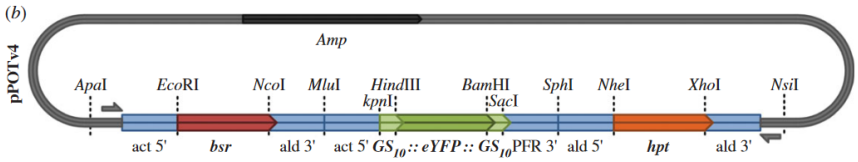

Figure 5: pPOTv4 plasmid structure. "From 5′ to 3′: a unique forward primer binding site, *actin* 5′ UTR (shown in blue), *blasticidin S deaminase* (*bsr*) gene (shown in red), *aldolase* 3′ UTR (shown in blue), *actin* 5′ UTR (shown in blue), *GS (10): eYFP:GS (10)* (shown in green), *PFR2* 3′ UTR (shown in blue), *aldolase* 5′ UTR (shown in blue), *hygromycin phosphotransferase* (*hpt*) gene (shown in orange), *aldolase* 3′ UTR (shown in blue), a unique reverse primer binding site." (Dean et al, 2015).

3.4 Gibson Assembly

Gibson assembly describes a biological method joining DNA fragments with overlapping ends in a flawless and correct order. The reaction proceeds under constant temperature conditions and involves the activity of three different enzymes (Figure 6a). 5' exonuclease is utilized to initiate nucleotide removal to obtain single stranded nucleotide regions at the 5' end on both DNA fragments exhibiting overlapping ends. As these single stranded regions are complementary, strands can anneal and be extended in 3' direction by DNA polymerase, leaving nicks that are sealed by DNA ligase (Gibson et al., 2009).

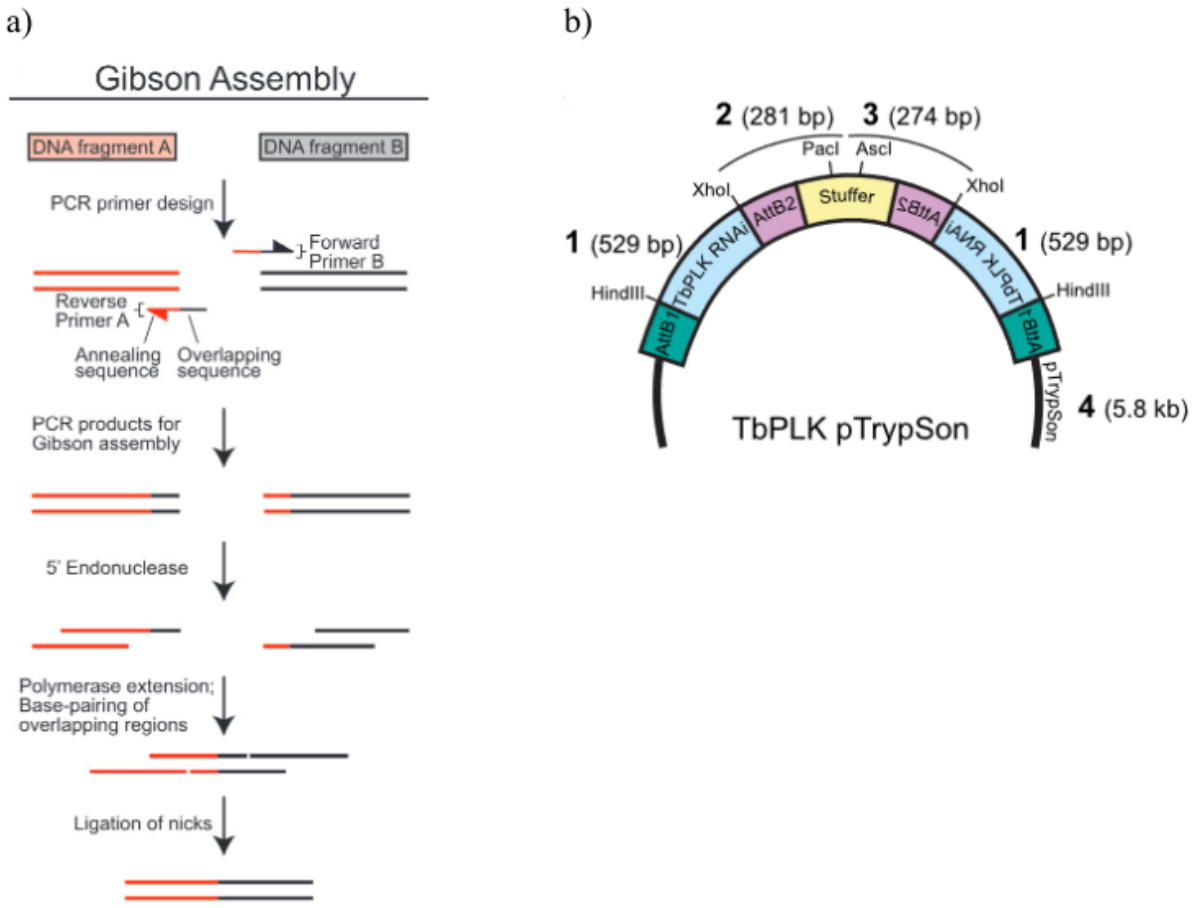

Figure 6: a) Gibson assembly reaction steps. 5' Endonuclease creates single stranded nucleotide regions at the 5' end on both DNA fragments followed by annealing of the strands. DNA polymerase then extends the annealed strands in 3' direction followed by ligation of nicks due to DNA ligase (Dean et al., 2016). b) TbPLK pTrypSon backbone structure, TbPLK RNAi sequence for triggering RNAi (1), a copy of AttB2 together with the first stuffer region (2), an inverted copy of AttB2 together with the second stuffer region (3), an inverted second copy of the gene sequence (1), and the tetracycline-inducible plasmid (4) (Dean et al., 2016).

Throughout this thesis Gibson assembly was performed with TbPLK pTrypSon plamid backbones (see Figure 6b) to generate long hairpin RNAi constructs. The segments to be inserted inside the plasmids were amplified by PCR over gDNA with overhanging primers homologous to the Attb1 and Attb2 sequences compromised within the stuffer and the plasmid. The Gibson assembly reaction was then performed with the HindIII-digested plasmid, the sequences compromised by the stuffer sections and the genes specific RNAi segments yielded the long hairpin RNAi constructs within one single reaction (Dean et al., 2016).

After sequencing confirming the correct hairpin assembly, vector digestion with the restriction enzyme NotI was performed, followed by transfection of the constructs into PCF *T. brucei* cell lines.

3.4 Transformation

Transformation is a biological process performed to help nucleic acids transverse throughout bacterial cell membranes and reach an intracellular site required for their further replication and expression. Transformation can either be carried out in a physical (due to pores within the membranes) or chemical manner (due to a state of competence) (Sambrook et al., 1989). Throughout this project, the transformation procedure was performed by using the heat shock method. Thereby cells are made competent due to a calcium-rich environment resulting in the compensation of repulsive forces between the genetic fragments and the host cell membranes (Chang et al., 2017). By heat-shocking these competent cells, pores within the cells' membranes are created as a pressure difference between the cells' interior and exterior arises throughout this process, allowing plasmid DNA to enter. Upon cooling cells to average temperatures again within non-antibiotic-containing media, cells are allowed to self-heal, followed by plating them on antibiotic-containing LB agar plates to obtain colony growth (Chang et al., 2017). Afterward, screening can be performed based on colony PCR to evaluate the proper expression/assembly of the plasmid within competent cells.

For transforming the Gibson assembly product into *E. coli* XL-1 Blue bacteria approximately 3 µL of each obtained Gibson assembly product was mixed with 50 µL XL-1 Blue bacteria followed by incubation on ice for 30 minutes (min). Bacteria were then subjected to heat shock at 42°C for 40 seconds and placed on ice for 5 min to increase inoculation efficiency. The bacterial transformation mixes afterward were incubated at 37°C for an hour in 1 mL of LB media allowed to recover while shaking. Samples then were centrifuged at 3000 rpm for 10 min, 200 ul of the resuspended pellet were plated onto ampicillin Petri dishes and incubated overnight at 37°C. The obtained colonies were screened for the presence of insert by Colony PCR.

3.5 Agarose gel electrophoresis

Agarose gel electrophoresis is a biological method that separates, identifies, and purifies DNA and RNA fragments. The samples thereby are separated within a gel agar matrix. Due to their negatively charged phosphate backbones, sample movement towards the positively charged cathode results from applied electric currents to the gel. During separation, taller molecules are retained more within the gel matrix than smaller ones and thus migrate slower. Visualization of the separated molecules is performed based on stains within the gels like ethidium bromide or SYBR Green (Yılmaz et al., 2012).

Throughout this project, 1% w/V gels for an agarose gel electrophoresis were made by weighing 0.8 g of solid Agarose and adding 1x TAE buffer to a final volume of 80 mL. In addition, ethidium bromide was added to a final concentration of 0,5 µg/mL.

After gelation, the gel was transferred into the electrophoresis chamber filled with 1x TAE buffer. The samples were supplemented with 6x loading buffer (NEB) and loaded into the gel. Electrophoresis was performed at 100-110 V for approximately an hour. Visualization of the gel was performed by UV illumination under the ChemiDoc XRS+ Gel Imaging System using the software ImageLab from BioRad.

3.6 Parasite cultures

All experiments were performed in procyclic *T. brucei* SMOX cells (Lister 427 strain) as a wild type strain. Cells cultivation was performed at 27°C in T-25 culture flasks. Cells were kept growing under exponential phase of growth by diluting with SDM-79 media with dialyzed 10% bovine fetal serum (for components see appendix) mixed with the appropriate antibiotic.

3.7 Transfection of PCF T. brucei with the AMAXA Nucleofactor II (VPA-1002 Lonza)

In general, transfection consists of the introduction of foreign DNA into a eukaryotic/mammalian cell. Throughout this project, transfection was carried out by electroporation to obtain recombinant cell lines expressing either RNAi hairpins or tagged protein products. Therefore, host cells together with the selected molecules were resuspended within a conductive solution. By applying electric pulses to this mixture, the phospholipid bilayers within the cell membranes are getting disrupted and giving rise to temporary pores. As the electric membrane potential rises within this process, charged molecules can transfer into the cell's interior throughout these pores (Weaver, 2000). As soon as no further pulses are applied to the cell mixture, pores will close again, producing recombinant cell lines.

To obtain recombinant cell lines, $5x10^7$ PCF *T. brucei* SMOX cells were harvested for transfection by spinning them down at 1300 x rcf and 4°C for 10 min. After centrifugation, the cell pellet was resuspended in 100 uL of Amaxa transfection mix (81,8 uL of Human T-Cell Nucleofactor supplemented with 18,2 uL of Supplement 1). Resuspended cells were mixed with 10-12 µg of NotI linearized DNA, placed into a gap cuvette provided in Amaxa™ Human T Cell Nucleofector™ Kit (Lonza), and electroporated in the AMAXA machine (Nucleofector™ II, Lonza) under the program X-014. After transfection, cells were placed into a culture T-25 flask containing 6 ml SDM-79 media and incubated for 16-18 hours or overnight at 27°C.
After this incubation, 6 mL of SDM-79 media with 10% FBS containing either hygromycin (for tagging cell lines) or hygromycin and phleomycin (for RNAi cell lines) antibiotic at 2x concentration was added to the flask (final concentration: 50 µg/mL of hygromycin, 25 µg/mL of phleomycin).
This mixture was then diluted within a 24 well plate to facilitate the cloning of transfectants.

3.8 Immunofluorescence assay

IFA is a biological method that evaluates specific epitopes within protein mixtures extracted from eukaryotic cells. It works due to interactions between epitopes and specific antibodies. By IFA investigations, conclusions about the presence of the epitope within the cells and assumptions about its subcellular localizations within the cells can be performed. Throughout this project, indirect IFA investigations were used in which a primary antibody is specifically binding to the epitope of interest. This epitope-antibody complex is then bonded by a fluorophore-labelled secondary antibody, which is possible to be detected and evaluated by microscopy.

To visualize and evaluate the localization of the selected proteins within *T. brucei* cells, IFA investigations were performed. Therefore, cells were harvested, and a 2x washing step (each time 900 g, 5 min, RT) with 1 mL vPBS (Voorheis's-modified phosphate-buffered saline (PBS) supplemented with 10mM glucose and 46mM sucrose, pH 7.6) was performed. Cells were resuspended in 200-400 µL vPBS, and 20 µL of the cell suspension was transferred to a microscopic slide covered with poly-L-lysine. After an incubation period of 10 min, the remaining liquid with non-attached cells got replaced with 4% paraformaldehyde, and cells were fixed for another 15 min at RT. After fixation, cells were permeabilized with 0.1% Triton X-100 in PBS (TX-100) for 15 min, followed by blocking for one hour in 1% BSA in PBS supplement with 0.033% TX-100 and exact concentration of TX-100 was also used for washing steps (but without BSA). Monoclonal mouse α-mtHsp70 antibody (Heat Shock Protein 70) was utilized as a mitochondrial marker. Rabbit α-V5 was used for V5 tagged proteins. Incubation was done overnight with the corresponding antibodies at 1:1000 dilution.
The next day 3x washing steps in washing buffer was performed, and the incubation in secondary antibodies (goat α-rabbit Alexa Fluor 488 and goat α-mouse Alexa Fluor 555 both Life Technologies (dilution 1:1000)) was carried out. To eliminate the antibodies' unspecific binding of the antibodies 3x washing steps in washing buffer were completed, and DNA was stained with ProLong Gold antifade reagent with DAPI (Molecular Probes). Following observations were performed with a Zeiss fluorescence microscope Axioplan 2 equipped with an Olympus DP73 digital camera. Images were processed by ImageJ (Schindelin et al., 2012).

3.9 Sample Preparation for SDS-PAGE and Western Blot

3.9.1 Total lysate preparation

Cells with a concentration of approximately $1*10^7$ cells/mL were harvested by spinning them down at 900 xg for 3 min. Next, cell pellets were directly resuspended in Laemmli buffer. Lysates afterward were heated at 95°C for 5 min and loaded into the gel.

3.9.2 Cytoplasm-mitochondria fractionation

For a more precise and detailed localization determination of our proteins, cell organelle sample fractions were created. Therefore PCF *T. brucei* cells (around 4mL of cell line media) were harvested at 1000 x g and 4°C for 10 min. The supernatant of the sample was discarded, cell pellets were washed twice in PBS and were resuspended in 500 µL ice-cold lysis buffer. Then, 100 µL out of the total 500 µL suspension mix were transferred to a separate tube labelled WCL (whole cell lysate). The remaining 400 µL were mixed with 16 µL of digitonin to obtain a final 0.4mg/mL concentration. Cells were vortexed and incubated at RT for 5 min. Tubes then were spined at 14000 g and RT for 2 min. The obtained supernatant was stored on ice and labelled as CYT (cytoplasmic fraction). The remaining cell pellets again were washed in lysis buffer. Afterward, they were resuspended in fresh 400 µL of lysis buffer upon adding 4 µL Triton - X100 to obtain a final concentration of 0.1%. Samples were then incubated on ice for 5 min and labeled as MITO (mitochondrial) fraction.
The obtained fractionations were used for further SDA PAGE and Western Blot analysis.

3.10 SDS-PAGE (Sodium Dodecyl Sulphate-Polyacrylamide Gel Electrophoresis)

SDS PAGE is a biological separation technique utilized for protein separation. Sodium dodecyl sulphate (SDS) thereby is binding to the fragment backbones in a molar ratio resulting in protein denaturation. Together with another reducing agent, SDS is furthermore breaking the disulphide bonds within protein structures and thereby resulting in protein unfolding. Samples are thus transferred into negatively charged polypeptide chains with charges proportional to their chain length. If an electric current is then applied to these samples, separation is obtained. Negatively charged molecules thereby are migrating towards the positively charged cathode, like in agarose gel electrophoresis, whereby taller molecules are being stronger retained by the pores within the gel matrix than smaller ones, resulting in slower molecule movement (Sharma & Rajput, 2015).

Proteins from total lysates or subcellular fractions were separated by SDS Page electrophoresis prior to Western Blot analysis. Therefore, SDS PAGE gels were made (components and concentrations in appendix) and transferred into the electrophoresis chamber filled with running buffer (appendix). Samples then were loaded into the gel, and a voltage of 110V was applied for approximately 90 min to obtain protein separation.

3.11 Western Blot

Western Blot is a procedure applied on beforehand separated proteins by SDS-PAGE. During Western Blot investigations, these separated proteins are electroblotted onto membrane composed out of nitrocellulose or polyvinylidene difluoride (Kurien & Scofield, 2006). The membrane thereby absorbs the proteins without destroying their biological properties throughout the transferring or blotting process. Afterward, the membranes are treated with a blocking solution to obtain homophobic binding of the proteins onto the membrane. After sufficient binding of the proteins, the membrane is treated with antibodies to evaluate the presence of the desired epitope within the separated molecules. Therefore, a primary antibody is applied, explicitly binding the protein of interest, and forming an antigen-antibody complex. After sufficient washing of the membrane to get rid of unspecific binding, a fluorophore-labelled secondary antibody is applied, binding to the beforehand obtained antigen-antibody complex, which can be used for further epitope detections (Kurien & Scofield, 2006).

For a Western Blot analysis, a blotting buffer, a running buffer, a blocking milk (5% m/V milk in PBS 0,05% V/V Polysorbate 20), and a Polysorbate 20 0,05% V/V solution were prepared (see appendix for composition of solutions).

Sufficient transference of the beforehand SDS-PAGE separated proteins onto methanol activated polyvinylidene difluoride (PVDF) membranes was obtained by placing sponges as well as the filter papers in blotting buffer and packing them together with the membrane and the gel as indicated in Figure 7.

Membranes were blotted at 110 V for around 1.10 h-1.15 h, after which a blocking step for one hour in blocking milk was followed to prevent unspecific binding and reduction of background signals. Afterwards membranes were incubated in primary antibody overnight (V5 antibody for the tagged proteins, HSP70 as mitochondrial control, Adenine phosphoribosyl transferase (APRT) as cytoplasmic control, for dilution of antibodies see appendix).

The next day the membrane was washed 5x in PBS with Polysorbate 20 for 5 min each, followed by incubation in blocking milk together with the secondary antibody in the appropriate concentration for an hour. Afterwards membranes were washed 5x in PBS for 5 min to get rid of not yet bounded substances from the membrane. Visualization of the proteins was performed in the ChemiDoc XRS+ Gel Imaging System by using the software ImageLab from BioRad after applying ECL substrate (Clarity Western ECL Substrate from BioRad).

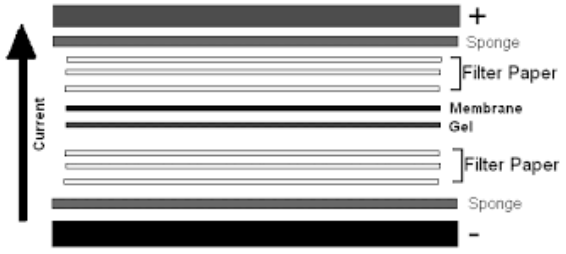

Figure 7: Blotting arrangement for transferring the proteins of the SDS PAGE onto the membrane.

3.12 RNA interference/ Growth curve

RNA interference (RNAi) describes the homology-dependent mechanism of controlling gene activity and expression by utilizing small double-stranded RNA molecules known as interfering RNA (Aagaard & Rossi, 2007). Generally, an RNAi procedure can be separated into three steps. Firstly, taller double-stranded RNA molecules within the cell are cut into several smaller pieces due to ribonuclease enzymes. Secondly, the obtained small RNA molecules are separated into single stands whereby the RISC complexes incorporate the leading strands. The incorporated leading strands can then activate the enzyme complexes resulting in the splicing of an mRNA molecule compromising complementary sequence to the leading strand. Based on this process, the leading strand determines which mRNA is spliced and in which way. Alternatively, the enzyme complex can block mRNA molecules with complementary sequences to the leading strand as information carriers without splicing them due to simple cleavage (Sharma & Rao, 2009). In both ways, the genetic information of the spliced or cleaved sequence is not being translated into a protein and thus resulting in its loss of function or downregulation of the protein.

Throughout this project, tetracycline-inducible RNAi cell lines were used to establish the proteins' function. As *T. brucei* maintained the structure required for RNAi investigations, uncomplicated loss of function experiments could be performed (McAllaster et al., 2016).

Therefore, transfected RNAi cultures were seeded at $1x10^6$ cells/mL and induced by adding 1 µg/mL tetracycline daily. Cells were maintained at 27°C and counted every 24h to screen the cell lines' growth behaviour and plot a growth curve. Western Blot investigations were performed to evaluate the inhibition or downregulation of the selected proteins within the cell line, for which probes were collected daily over a specific time range during induction.

4 Results

4.1 Endogenous gene tagging and pTrypson RNAi construct generation

For creating PCF *T. brucei* V5 tagged cell lines as well as RNAi cell lines for our selected proteins endogenous tagging and molecular cloning was performed.

Molecular sizes of the obtained PCR fragments afterwards were evaluated by agarose gel electrophoresis.

4.1.1 Endogenous Tagging Results

As template for the tagging long primer PCR, modified pPOT vectors containing V5 tag were used. PCR products compromising the long primer amplicon for Tb927.2.5020, Tb927.6.1570 and Tb927.8.1440 were immediately obtained after performing long primer PCR once. For Tb927.8.6970 the reaction procedure needed to be repeated another three times till a corresponding long primer amplicon was obtained. Agarose gel pictures as well as the corresponding sizes of each of the selected proteins are shown in Figure 8.

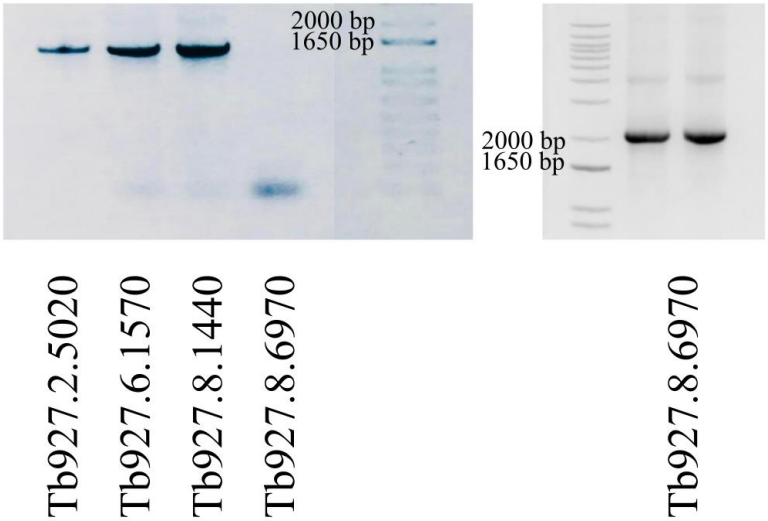

Figure 8: Agarose gel electrophoresis pictures of V5 tagged Tb927.2.5020, Tb927.6.1570, Tb927.8.1440 and Tb927.8.6970. Each of the prioritized molecules compromised a molecular weight between 1650 bp and 2000 bp

The obtained PCR amplicons were then recombined and further used in transfection reactions to obtain PCR *T. brucei* tagged cell lines for each protein (performed by supervisor). Transfections for all the selected proteins worked immediately and the obtained cell lines were used for further subcellular localization determination experiments.

4.1.2 Generation of PCF T. brucei RNAi Cell Lines

To create RNAi constructs for obtaining PCF *T. brucei* RNAi cell lines, PCR over gDNA was performed followed by Gibson assembly and transformation of the obtained RNAi constructs into *E. coli* XL-1blue bacteria.

PCR reactions of the gene regions of interest needed to be performed twice till products for all the selected proteins were obtained. The obtained PCR products were all evaluated by agarose gel electrophoresis to investigate their molecular weights (see Figure 9).

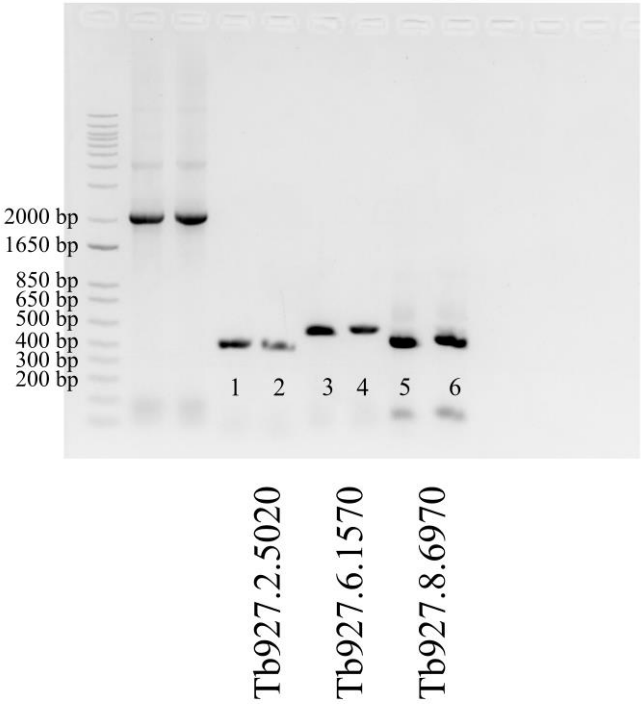

Figure 9: evaluation of the long primer PCR reaction by agarose gel electrophoresis. Slots 1 and 2 showing product bends for Tb.927.2.5020, 3 and 4 for Tb927.6.1570, 5 and 6 for Tb927.8.6970. All proteins had molecular weights of 400 to 500 bp.

PCR products were then further processed by Gibson assembly followed by transformation of the constructs into *E. coli* XL-1 blue bacteria. The obtained colonies were further screened for the proper expression of inserts by colony PCR and were evaluated by agarose gel electrophoresis. As Gibson transformation of Tb927.2.5020 went wrong, we only obtained colonies for the remaining proteins (1 colony for Tb.927.6.1570, 17 for Tb927.8.1440 and 34 for Tb927.8.6970).

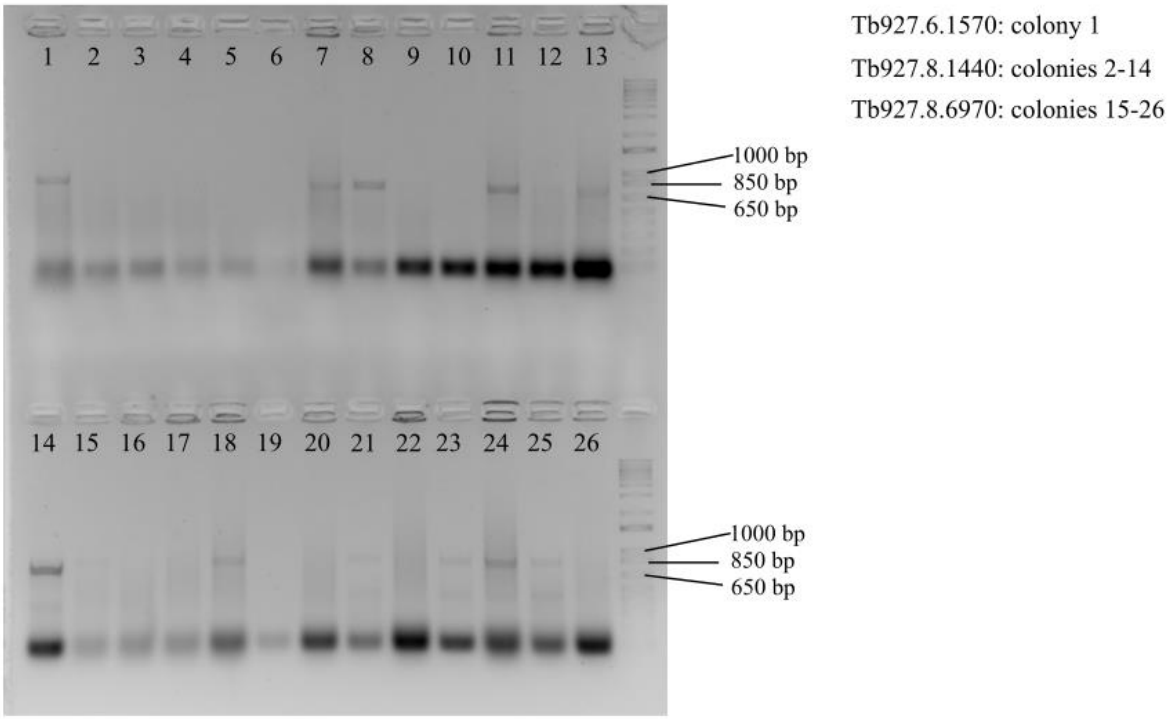

Figure 10: agarose gel evaluation of the performed colony PCR for Tb927.6.1570, Tb927.8.1440 and Tb927.8.6970. Throughout transformation 1 colony for Tb927.6.1570 was obtained for screening. Colonies 2-14 were obtained and screened for Tb927.8.1440. Screened colonies 15-26 belong to Tb927.8.6970. Colonies 1,8,11,14 and 18 were cultivated for further investigations.

Based on the electrophoresis results (see Figure 10) from the first performed colony PCR, colonies 1,8,11,14 and 18 were cultivated and purified. pTrypSon plasmid linearization was performed due to restriction enzyme activity (NotI). As correct sizes of the products in further Agarose gel electrophoresis could not be verified, samples were discarded. Therefore, Gibson re-transformation for Tb927.2.5020 and Tb927.6.1570 was performed to obtain colonies for screening, whereas for Tb927.8.1440 and Tb927.8.6970 the remaining colonies were used.

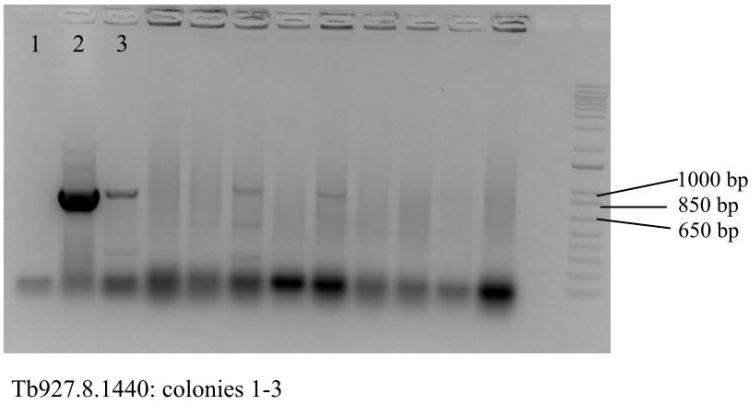

Figure 11: Colony PCR screening results for Tb927.8.1440. In total three colonies were screened which are labeled correspondingly within the picture.

For Tb927.8.1440 three colonies were further screened, from which 2 seemed to contain the properly inoculated and expressing plasmid with the corresponding insert (see Figure 11). Colonies 2 and 3 were cultivated, purified, and linearized. The further performed agarose gel electrophoresis proved the correct sizes of products which then were send for further sequencing. As the sequencing results of colony 3 were in accordance with the expected data, the purified product was used for transfection yielding in the corresponding PCF *T. brucei* RNAi cell line.

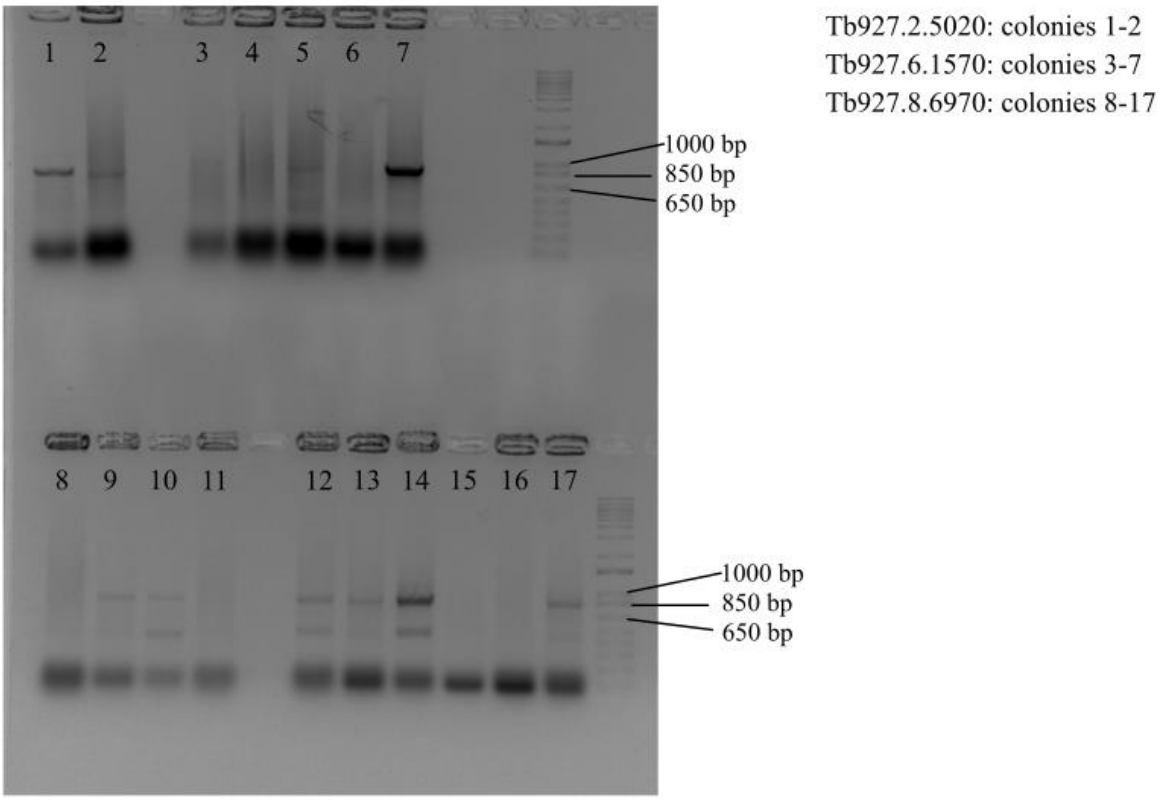

Figure 12: Colony PCR screening results for Tb927.2.2050, Tb927.6.1570 and Tb927.8.6970. Colonies 1 and 2 belong to Tb927.2.5020, colonies 3-7 belong to Tb927.6.1570 and colonies 8-17 to Tb927.8.6970

For the remianing proteins screening was re-performed as well (see Figure 12). As only colony 1 for Tb927.2.5020 and colony 7 for Tb927.6.1570 seemed to contain the plasmids with the correponding inserts both of them were cultivated, purified and linearized. Sequencing reults veryfied the correct seqeunces and tranfection reactions were tried to be performed (performed by supervisor). However no corresponding RNAi cell ines were obtained and thus no knockdown studies could be performed.

4.2 Tagging and subcellular localization analysis of prioritized candidates

For all prioritized proteins the perfomed whole cell lysate V5 Westen Blot investigations indicated that the tagged genes were succesfully introduced and transfected into PCF *T. brucei* cell lines, as the corresponding sizes were the expected (see Figure 13). Results were obtained independently in seperated Western Blot invstigations and are thus shown seperately.

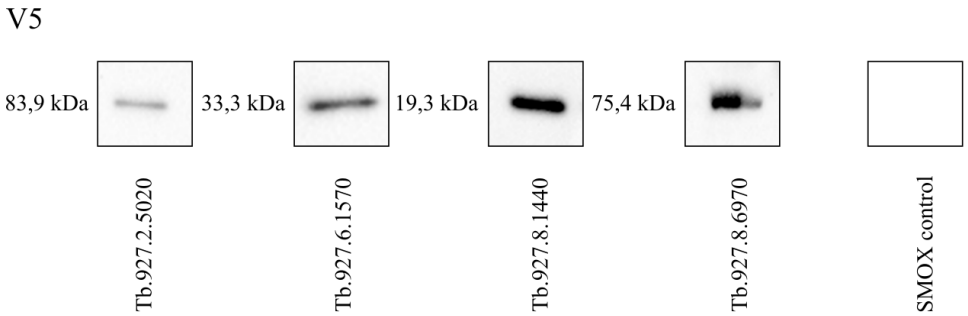

Figure 13: whole cell lysate V5 Western Blot results for Tb.927.2.5020, Tb.927.6.1570, Tb.927.8.1440, Tb.927.8.6970 and SMOX control. Molecular weights for all proteins are indicated in kliodaltons.

The subcellular localization of the prioritized gene products was assessed by IFA rendering the results depicted in Figure 14.

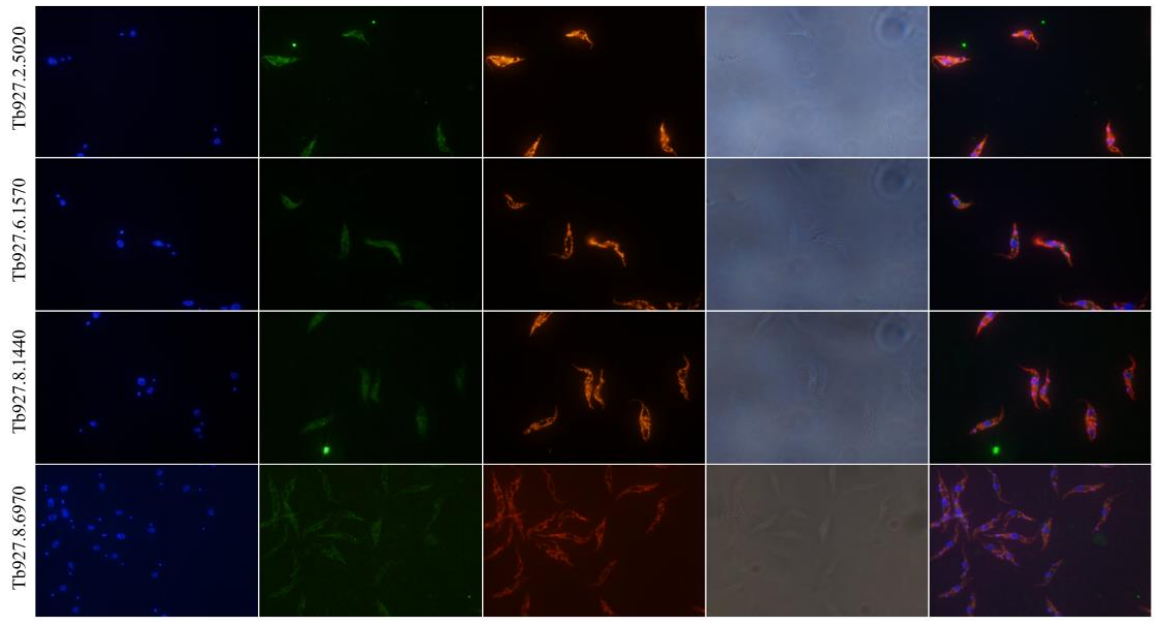

Figure 14: IFA pictures of prioritized proteins. Proteins were indicated by their corresponding GIs. DAPI within the first column displaying stained nucleic genetic material, V5 within the second column the V5 tagged selected proteins, HSP70 within the third column was used as mitochondrial marker. Furthermore, phase contrasts (fourth column) are provided to ensure normal cell shapes of the investigates cells. Composites within the last column are displaying the merge of the DAPI, HSP70 and V5 signal all together.

Throughout IFA experiments, a V5 antibody was used for detection of our tagged proteins, HSP70 was utilized as a mitochondrial marker, DAPI was used for staining and visualizing genetic material within the nucleus of the cell and the kinetoplast.

The V5 obtained signals showed in green have very low signal intensities in comparison to the HSP70 signal being much stronger. Overlaps of the V5 signal with the mitochondrial HSP70 marker only for Tb.927.2.5020 and Tb.927.8.6970 could be observed, while Tb.927.6.1570 and Tb.927.8.1440 displayed distinct subcellular localization results in contrast to the HSP70 signal.

Thus, based on the performed IFA investigations over procyclic cells a mitochondrial subcellular localization can be expected for Tb.927.2.5020 and Tb.927.8.6970. For Tb.927.6.1570 and Tb.927.8.1440 in contrast, as no overlap of the V5 tagging signal and the mitochondrial HSP70 signal could be observed, a cytoplasmic localization can be suspected.

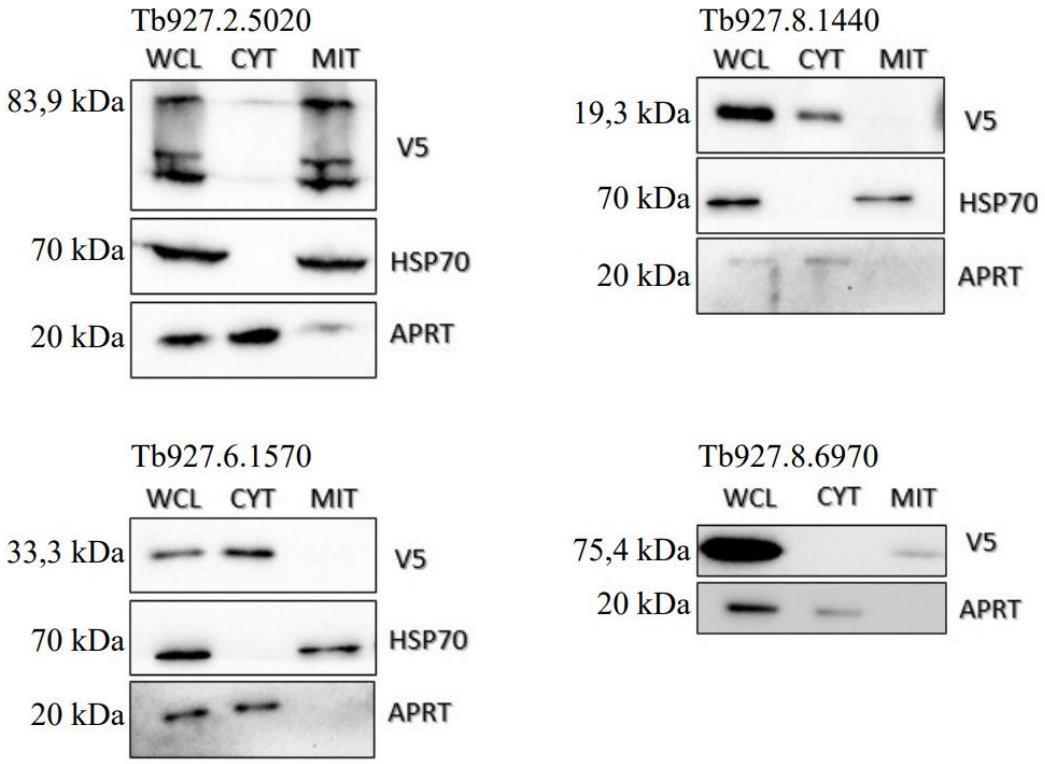

Figure 15: Cellular fractionation Western Blot results of Tb.927.2.5020, Tb.927.6.1570, Tb.927.8.1440 and Tb.927.8.6970, WCL: whole cell lysate, MIT: mitochondrial fractionation, CYT: cytoplasmic fractionation, HSP70: mitochondrial control, APRT: cytoplasmic control, V5: V5 tagged protein. Molecular weighta are indicated in kilodaltons (kDa) next to the signas.

The aim of performing Western Blot over cellular fractionations for Tb927.2.5020, Tb927.6.1570, Tb927.8.1440 and Tb927.8.6970 was to obtain another line of evidence to assess their localizations (see Figure15). As a mitochondrial marker HSP70 was used. Cytoplasmic subcellular localizations were evaluated by APRT. Both markers are bona fide markers of these compartments already used in several previous research investigations (Doleželová et al., 2021).

Based on the Western Blot results it can be concluded that proteins Tb927.2.5020 and Tb927.8.6970 have a mitochondrial subcellular localization. Tb927.6.1570 and Tb927.8.1440 instead seem to be cytoplasmic.

As in the IFA composites for Tb927.6.1570 and Tb927.8.1440 the obtained V5 signals are not completely overlapping with the red signals from the HSP70 marker, a cytoplasmic subcellular localization can be expected. Thus, Western Blot results are in good agreement with the results obtained by IFA for Tb927.6.1570 and Tb927.8.1440.

Furthermore, as for Tb927.2.5020 and Tb927.8.6970 the V5 and HSP70 signals are overlapping in IFA, and the obtained cellular fractionation Western Blot results for these gene products are as well indicating a mitochondrial subcellular localization, these results are also in good agreement to each other.

4.3 RNAi analysis of Tb.927.8.1440

We analysed the effects of RNAi ablation for Tb.927.8.1440. Based on the obtained RNAi cell line a growth curve was carried out (Fig. 16). Cells were stably transfected with the RNAi construct of Tb.927.8.1440 to assess the essentiality of the gene product.

No effects on the growth of *T. brucei*, due to ablation of Tb.927.8.1440 could not be observed. This is due to the lack of RNAi downregulation for this protein, as assessed by Western Blot analysis (see Figure 17).

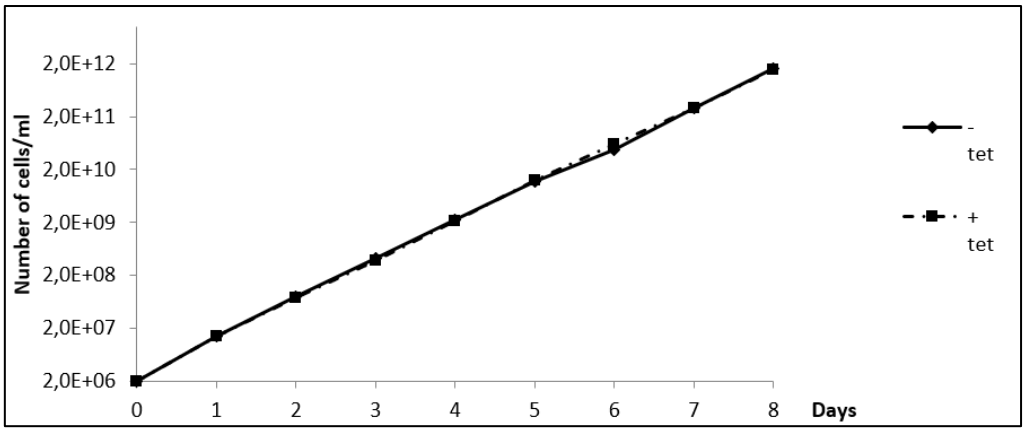

Figure 16: growth curve of RNAi construct from Tb.927.8.1440. Standard growth curve, the number of cells per mL is represented in an non induced (-)/induced (+) form with tetracycline over a time range from 9 days (day 0: start, day 8: end) No difference between the induced and non-induced form could be observed.

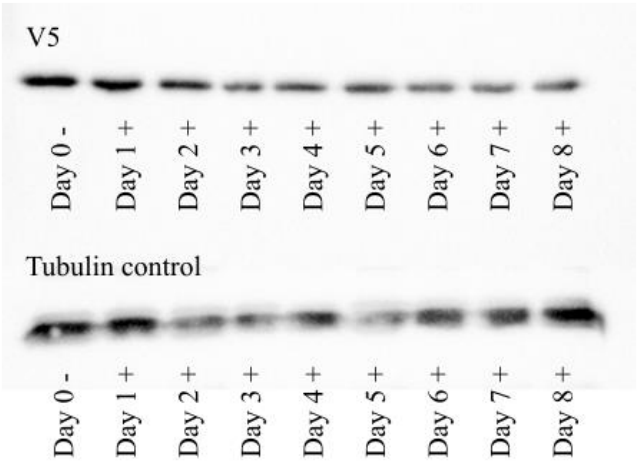

Figure 17: V5 and Tubulin Western Blot results for performed growth curve of Tb.927.8.1440 RNAi construct. Lines correspond to day 0-8, - indicating non induced with tetracycline, + indicating induced with tetracycline. Tubulin control serving as a loading control of samples.

As it is shown in the Western Blot performed to check downregulation of Tb.927.8.1440 (Figure 17) only a very low decrease of the protein expression could be observed over the time range of 8 days of RNAi induction with tetracycline, which is in good correlation with the lack of growth phenotype. This most probably be in turn due to lack of proper induction of RNAi expression. Higher concentrations of Tetracycline could be assayed to rule out this possibility

5 Discussion

To examine the dual localization findings of the TrypTag.org project regarding the proteins Tb.927.2.5020 (acyl-CoA oxidase), Tb.927.6.1570 (2-hydroxy-3-oxopropionate reductase), Tb.927.8.1440 (maoC-like dehydratase), and Tb.927.8.6970 (3-methylcrotonyl-CoA carboxylase) immunofluorescence microscopy as well as Western Blot with crude cellular fractionations over appropriate mitochondrial and cytoplasmic controls of the cell lines were carried out. To verify our obtained localization results under a lower degree of uncertainty, references towards other previously performed studies within the mito- and glycoproteomic area of *T. brucei* were performed.

To evaluate our mitochondrial localization results for Tb927.2.5020 and Tb927.8.6970, available data mapping the mitochondrial proteomes of PCF as well as of BSF based on mass spectroscopy was consulted (Zíková et al., 2017). This data did not only prove that the mitochondrial proteome of BSF *T. brucei* cells is approximately reduced by 20% in comparison to the mitoproteome present within PCF cells, but it also interestingly detected all four of our selected proteins within the mitochondria. As this is in accordance with our localization results for Tb927.2.5020 and Tb927.8.6970, they could indeed exhibit a mitochondrial subcellular localization (Zíková et al., 2017).

Further investigations were performed to confirm our subcellular localization results of Tb927.8.1440 and Tb927.6.1570. As it was proven that under low-glucose conditions, mislocalization of glycosomal matrix proteins is more supported and that they thus can be detected in the cytoplasm prior to import into the glycosome (Bauer & Morris, 2017), a possible glycosomal relation of our proteins is needed to be evaluated. Therefore, data investigating the glycosmic proteome within PCF *T. brucei* cell lines was reconciled, which used magnetic bead enrichment, epitope tagging as well as SILAC quantitative proteomics to determine a high confidence glycosomic proteome of *T. brucei* (Güther et al., 2014). By using isotope ratios, differentiation between glycosomal from mitochondrial and other contaminating proteins could be made thus that throughout antiepitope pull-out experiments, genuine glycosomal components could be separated from other contaminations according to peptide isotopic signatures (Güther et al., 2014).

For Tb927.8.1440 and Tb927.6.1570, a possible glycosomal relationship could be reported based on these experiments (Güther et al., 2014).

Thus Tb927.8.1440 and Tb927.6.1570 could eventually as well exhibit a glycosomal subcellular localization in contrast to our obtained cytoplasmic localization results, and further investigations towards their true subcellular localization should be carried out.

Further research perspectives towards a possible glycosomal relation could include performing experiments under distinct glucose levels and utilizing different crude cellular digitonin fractions with appropriate glycosomal markers.

6 Conclusion

The main goal of this thesis was to localize Tb927.2.5020 (acyl-CoA oxidase), Tb927.6.1570 (2-hydroxy-3-oxopropionate reductase), Tb927.8.1440 (maoC-like dehydratase), and Tb927.8.6970 (3-methylcrotonyl-CoA carboxylase) in PCF *T. brucei* cell lines. To examine the dual localization findings of TrypTag.org regarding the selected proteins immunofluorescence microscopy as well as Western Blot analysis with crude cellular fractionations over appropriate controls of the cell lines were carried out.

In contrast to the performed procedures from TrypTag.org, the selected proteins were only C-terminally tagged instead of tagging them at both termini. Also, mNG, a bulky reporter protein, was exchanged by the smaller V5 tag to prevent possible artefactual subcellular mislocalization signs. CT tagging was preferred over NT tagging due to the possibility of interfering with targeting signal peptides located at the NT and thus eventually generating wrong localization results.

Differently than stated by TrypTag.org, mitochondrial non-TAC-related subcellular localizations for Tb927.2.5020 and Tb927.8.6970 were detected within our IFA and Western Blot investigations when tagging the proteins CT by V5. For the proteins, Tb927.6.1570 and Tb927.8.1440, in contrast, a cytoplasmic localization was observed within Western Blot analysis, which is in accordance with the localization data provided by TrypTag.org. As well as for the beforehand mentioned proteins, no point localization when tagged by V5 for Tb927.6.1570 and Tb927.8.1440 could be observed by IFA analysis, and thus, no TAC related localizations were verified.

Based on our obtained results and by comparing them to previously performed research within the mitoproteomic and glycoproteomic area of *T. brucei*, we concluded that Tb927.2.5020 and Tb927.8.6970 indeed could exhibit a mitochondrial localization. Tb927.8.1440 and Tb927.6.1570, in contrast, are either exhibiting a cytoplasmic or glycosomal localization.

Knockdown studies of Tb927.8.1440 were performed by using long hairpin RNAi. The V5 tagged maoC-like dehydratase RNAi cell line showed either none or a very small decrease of the protein observed by Western Blot during the induction of RNAi with tetracycline. This agreed with the obtained growth curve in which no specific growth phenotype could be assessed. Therefore, no clear prediction of the essentiality of this protein within the cell could be made.

Appendix

Primer sequences

Tb927.2.5020	TAG	AAGAGAAGATGGAGGAATCAAGGGAAGATTTTGATCTTTTCCATGGGCTAGCGGGCAAACAGTCCTTTGCACAAGAGAAAGGTTCTGGTAGTGGGTTCC	acyl-CoA oxidase, putative
Tb927.2.5020		CAGGGGATACCAAATTTTCACACGAGTGCGCACTGAAAAAAGAAAAAGAAAGAATCAAGCGATTGAAGTAGTTGAATGCACCAATTTGAGAGACCTGTGC	acyl-CoA oxidase, putative
Tb927.6.1570		GCGAAGGTGATTTGGACAACTCTGCTATCATTGGCGTGTTAGAGCGCATGGCCAACTGCAAGATTAAGGAGACCAAGCCAGGTTCTGGTAGTGGTTCC	2-hydroxy-3-oxopropionate reductase, putative
Tb927.6.1570		AAAAATGCCCATGTGCGTGTGCGTATGCGTTTGTTGAAAACGACAAACAGTTACCGATCTGAGGATGATTGGGGAGATTGCCAATTTGAGAGACCTGTGC	2-hydroxy-3-oxopropionate reductase, putative
Tb927.8.1440		GTATCGAAGGCACTGCGGTGGGCATGAACAAGACAGTTACCTTTGAAGGTGAGAGCGAGTGGAATGTGCCCCGTGTCGAGGGTTCTGGTAGTGGTTCC	maoC-like dehydratase, putative
Tb927.8.1440		CCCCCAACGCTCCCAAAACAAGAAGACGAGAAAATGCAAAACGGTACGGCACAACCTCCTTTCTTCGTTAACGTCAAACGCCAATTTGAGAGACCTGTGC	maoC-like dehydratase, putative
Tb927.8.6970		GAGAGGTGAAGTTTTGCGTTCATGCAGATGGCATAGTCGGAGGAAGCACTTTACTTGCCCATATTGCCTCTGCTGCAGTTGGTTCTGGTAGTGGTTCC	3-methylcrotonyl-CoA carboxylase alpha subunit, putative
Tb927.8.6970		TGTGGATGGCGCTGCACAGGGCAAGGAAAACAAAACCGGTTGAAGGCCCCTACAACTTGCAGTCGAAGCGCCTCTAAGCTCCAATTTGAGAGACCTGTGC	3-methylcrotonyl-CoA carboxylase alpha subunit, putative
Tb927.2.5020	RNAi	ACAAGTTTGTACAAAAAAGCAGGCTAAGCTTGCGAGGCCGATTAATGGAGA	acyl-CoA oxidase, putative
Tb927.2.5020		ACCACTTTGTACAAGAAAGCTGGGTCTCGAGGAAGTACAGGGTTCCGGCAA	acyl-CoA oxidase, putative
Tb927.6.1570		ACAAGTTTGTACAAAAAAGCAGGCTAAGCTTCGTCGATGTCGTCTTCACCA	2-hydroxy-3-oxopropionate reductase, putative
Tb927.6.1570		ACCACTTTGTACAAGAAAGCTGGGTCTCGAGCCTCGCGGAATCCATTACGA	2-hydroxy-3-oxopropionate reductase, putative
Tb927.8.1440		ACAAGTTTGTACAAAAAAGCAGGCTAAGCTTCGGATCGGTGATTTTGCGTC	maoC-like dehydratase, putative
Tb927.8.1440		ACCACTTTGTACAAGAAAGCTGGGTCTCGAGACATTCCACTCGCTCTCACC	maoC-like dehydratase, putative
Tb927.8.6970		ACAAGTTTGTACAAAAAAGCAGGCTAAGCTTTATTTACGCCGAATCGCCGA	3-methylcrotonyl-CoA carboxylase alpha subunit, putative
Tb927.8.6970		ACCACTTTGTACAAGAAAGCTGGGTCTCGAGTGGAGACAGTGACACGAACG	3-methylcrotonyl-CoA carboxylase alpha subunit, putative

Reaction Mix for V5 protein tagging

Component	amount
Q5 hotstart	25 µL
water	23 µL
Corresponding forward primer	1 µL
Corresponding revers primer	1 µL
pPOTv5 (plasmid PCR only tagging)	0,5 µL

Primers for Colony PCR

gRNAi forward	CGCTGACTTTCCAAGACCTC
gRNAi reverse	CAGATCGTCTTCACCCCCTA

Reaction mix used for Gibson assembly to create long hairpin:

Components	Suggested amount	Used amount *
Stuffer	50-100 ng per reaction (2x excess)	0,75 µL
pTrypson	50-100 ng per reaction	0,1 µL
mQ water	1,15 µL	1,15 µL
Gibson Assembly Master mix	5 µL	5 µL

* Total volume of the mix should be 8,5 µL. To less water within the mixture, 2,65 µL were supposed to be added

Gibson assembly master mix composed out of 699 µl MilliQ H2O, 320 µl 5x isothermal reaction buffer [500 mM Tris-HCl, 250 mg/ml PEG–8000, 50 mM MgCl2, 50 mM DTT, 1 mM Each of four dNTPs], 0,64 µl T5 exonuclease, 20 µl phusion DNA polymerase, 160 µl Taq DNA ligase.

Composition of gels used for SDS-PAGE

Substance amounts for 1gel	Resolving gel (10 ml)	Stacking gel (6 ml)
Water	3.3 ml	4.35 ml
Acrylamide Mix	4.0 ml	1.0 ml
Tris buffer (1.5M)	2.5 ml	0.5 ml
SDS	0.1 ml	0.06 ml
APS (Ammonium persulphate)	0.1 ml	0.06 ml
N,N,N’,N’ Tetramethyl ethylenediamine	0.004 ml	0.006 ml

* Tris Buffer: resolving gel pH: 6.8, stacking gel pH: 8.8

Firstly, resolving gel was prepared and allowed to harden, afterwards liquid stacking gel was applied on top of the solidified resolving gel and as well allowed to harden.

Antibodies used for Western Blots:

Primary antibody	Dilution	Secondary antibody	Dilution
V5 made in mouse	1:1000	anti-mouse	1:1000
HSP70 in mouse	1:1000	anti-mouse	1:1000
APRT in rabbit	1:500	anti-rabbit	1:1000
α-Tubulin in mouse	1:1000	anti-mouse	1:1000

Solutions used for Western Blot:

Blotting buffer	
Water	700 mL
Methanol	200 mL
10x blotting buffer	100 mL

10x Blotting Buffer components for 2 liter	
192 mM Glycine	58 g
25 mM Tris	116 g
0,1% SDS	7,4 g

PBS + Polysorbate 20	
Water	900 mL
10x PBS	100 mL
Polysorbate 20	500 µL

Running Buffer	
Water	900 mL
10x running buffer	100 mL

10x Running Buffer components for 2 liter	
25 mM Tris	60 g
192 mM Glycine	288 g
0,1% SDS	20 g

Laemmli buffer (lysis buffer)

Reagent	Molecular weight	Concentration (M or %)
1x		
Tris base	121,14	0,0625 M
SDS	288,37	0,07 M (2%)
Glycerol	92,09	10%
2-mercapto-ethanol	78,13	5%
Bromophenol blue	691,94	-

Components of the SDM-79 medium for maintaining the parasite cultures:

SDM-CGGGPPTA	22,05 g
Sodium bicarbonate	2 g
Sodium acetate	10 mg
L-Glutamic acid	22 mg
L-Glutamine	500 mg
L-Proline	600 mg
L-Threonine	400 mg
Sodium Pyruvate	100 mg
Glucose	1 g (pH 7,3)
Glucosamine	50 mg
Hemin	0,75 ml
Pen-Strep	10 ml
Distilled H2O	Bring to 900 ml
FBS	100 ml

PCR conditions for tagging and long primer PCR:

98 °C	2’	
98 °C	20’’	15x
65 to 50 °C	30’’	
72 °C	2’	
98 °C	20’’	20x
50 °C	30’’	
72 °C	2’	
72 °C	2’	
4 °C	∞	

List of used literature

Aagaard, L., & Rossi, J. J. (2007). RNAi therapeutics: principles, prospects and challenges. *Advanced drug delivery reviews*, *59*(2-3), 75-86.

Aslett, M., Aurrecoechea, C., Berriman, M., Brestelli, J., Brunk, B. P., Carrington, M., ... & Wang, H. (2010). TriTrypDB: a functional genomic resource for the Trypanosomatidae. *Nucleic acids research*, *38*(suppl_1), D457-D462.

Baral, T. N. (2010). Immunobiology of African trypanosomes: need of alternative interventions. *Journal of Biomedicine and Biotechnology*, *2010*.

Barrett, M. P., Burchmore, R. J., Stich, A., Lazzari, J. O., Frasch, A. C., Cazzulo, J. J., & Krishna, S. (2003). The trypanosomiases. *The Lancet*, *362*(9394), 1469-1480.

Baudouin, H. C. M., Pfeiffer, L., & Ochsenreiter, T. (2020). A comparison of three approaches for the discovery of novel tripartite attachment complex proteins in Trypanosoma brucei. *PLoS neglected tropical diseases*, *14*(9), e0008568.

Bauer, S., & Morris, M. T. (2017). Glycosome biogenesis in trypanosomes and the de novo dilemma. *PLoS neglected tropical diseases*, *11*(4), e0005333.

Bílý, T., Sheikh, S., Mallet, A., Bastin, P., Pérez-Morga, D., Lukeš, J., & Hashimi, H. (2021). Ultrastructural Changes of the Mitochondrion During the Life Cycle of Trypanosoma brucei. *Journal of Eukaryotic Microbiology*, e12846.

Bonhivers, M., Landrein, N., Decossas, M., & Robinson, D. R. (2008). A monoclonal antibody marker for the exclusion-zone filaments of Trypanosoma brucei. *Parasites & vectors*, *1*(1), 1-8.

Brun, R., Blum, J., Chappuis, F., & Burri, C. (2010). Human african trypanosomiasis. *The Lancet*, *375*(9709), 148-159.

Chang, A. Y., Chau, V. W., Landas, J. A., & Pang, Y. (2017). Preparation of calcium competent Escherichia coli and heat-shock transformation. *JEMI methods*, *1*, 22-25.

Dean, S., Sunter, J. D., & Wheeler, R. J. (2017). TrypTag. org: a trypanosome genome-wide protein localisation resource. *Trends in parasitology*, *33*(2), 80-82.

Dean, S., Sunter, J., Wheeler, R. J., Hodkinson, I., Gluenz, E., & Gull, K. (2015). A toolkit enabling efficient, scalable and reproducible gene tagging in trypanosomatids. *Open biology*, *5*(1), 140197.

Gibson, D. G., Young, L., Chuang, R. Y., Venter, J. C., Hutchison, C. A., & Smith, H. O. (2009). Enzymatic assembly of DNA molecules up to several hundred kilobases. *Nature methods*, *6*(5), 343-345.

Güther, M. L. S., Urbaniak, M. D., Tavendale, A., Prescott, A., & Ferguson, M. A. (2014). High-confidence glycosome proteome for procyclic form Trypanosoma brucei by epitope-tag organelle enrichment and SILAC proteomics. *Journal of proteome research*, *13*(6), 2796-2806.

Hoffmann, A., Jakob, M., & Ochsenreiter, T. (2016). A novel component of the mitochondrial genome segregation machinery in trypanosomes. *Microbial cell*, *3*(8), 352.

Hoffmann, A., Käser, S., Jakob, M., Amodeo, S., Peitsch, C., Týč, J., ... & Ochsenreiter, T. (2018). Molecular model of the mitochondrial genome segregation machinery in Trypanosoma brucei. *Proceedings of the National Academy of Sciences*, *115*(8), E1809-E1818.

Kurien, B. T., & Scofield, R. H. (2006). Western blotting. *Methods*, *38*(4), 283-293.

Liu, B., Liu, Y., Motyka, S. A., Agbo, E. E., & Englund, P. T. (2005). Fellowship of the rings: the replication of kinetoplast DNA. *Trends in parasitology*, *21*(8), 363-369.

Maier, R.M., Pepper, I.L., and Gerba, C.P. (2000) Environmental Microbiology. Academic Press, San Diego.

McAllaster, M. R., Sinclair-Davis, A. N., Hilton, N. A., & de Graffenried, C. L. (2016). A unified approach towards Trypanosoma brucei functional genomics using Gibson assembly. *Molecular and biochemical parasitology*, *210*(1-2), 13-21.

Oberholzer, M., Morand, S., Kunz, S., & Seebeck, T. (2005). A vector series for rapid PCR-mediated C-terminal in situ tagging of Trypanosoma brucei genes. *Molecular and biochemical parasitology*, *145*(1), 117-120.

Ogbadoyi, E. O., Robinson, D. R., & Gull, K. (2003). A high-order trans-membrane structural linkage is responsible for mitochondrial genome positioning and segregation by flagellar basal bodies in trypanosomes. *Molecular biology of the cell*, *14*(5), 1769-1779.

Panigrahi, A. K., Ogata, Y., Zíková, A., Anupama, A., Dalley, R. A., Acestor, N., ... & Stuart, K. D. (2009). A comprehensive analysis of Trypanosoma brucei mitochondrial proteome. *Proteomics*, *9*(2), 434-450.

Parsons, M. (2004). Glycosomes: parasites and the divergence of peroxisomal purpose. *Molecular microbiology*, *53*(3), 717-724.

Sambrook, J., Fritsch, E. F., & Maniatis, T. (1989). *Molecular cloning: a laboratory manual* (No. Ed. 2). Cold spring harbor laboratory press.

Schindelin, J., Arganda-Carreras, I., Frise, E., Kaynig, V., Longair, M., Pietzsch, T., ... & Cardona, A. (2012). Fiji: an open-source platform for biological-image analysis. *Nature methods*, *9*(7), 676-682.

Schnarwiler, F., Niemann, M., Doiron, N., Harsman, A., Käser, S., Mani, J., ... & Schneider, A. (2014). Trypanosomal TAC40 constitutes a novel subclass of mitochondrial β-barrel proteins specialized in mitochondrial genome inheritance. *Proceedings of the National Academy of Sciences*, *111*(21), 7624-7629.

Schneider, A., & Ochsenreiter, T. (2018). Failure is not an option–mitochondrial genome segregation in trypanosomes. *Journal of cell science*, *131*(18), jcs221820.

Sharma, R., & Rajput, Y. S. (2015). SDS-PAGE–Principle and Applications. *Advanced Techniques and Novel Approaches for Quality and Safety Evaluation of Dairy Foods*, 36.

Sharma, S., & Rao, A. (2009). RNAi screening: tips and techniques. *Nature immunology*, *10*(8), 799-804.

Trikin, R., Doiron, N., Hoffmann, A., Haenni, B., Jakob, M., Schnaufer, A., ... & Ochsenreiter, T. (2016). TAC102 is a novel component of the mitochondrial genome segregation machinery in trypanosomes. *PLoS pathogens*, *12*(5), e1005586.

Weaver, J. C. (2000). Electroporation of cells and tissues. *IEEE transactions on plasma science*, *28*(1), 24-33.

Yılmaz, M., Ozic, C., & Gok, İ. (2012). Principles of nucleic acid separation by agarose gel electrophoresis. *Gel Electrophoresis–Principles and Basics*, *4*, 33.

Zhao, Z., Lindsay, M. E., Roy Chowdhury, A., Robinson, D. R., & Englund, P. T. (2008). p166, a link between the trypanosome mitochondrial DNA and flagellum, mediates genome segregation. *The EMBO journal*, *27*(1), 143-154.

Zíková, A., Verner, Z., Nenarokova, A., Michels, P. A., & Lukeš, J. (2017). A paradigm shift: The mitoproteomes of procyclic and bloodstream Trypanosoma brucei are comparably complex. *PLoS pathogens*, *13*(12), e1006679.

List of figures